Scientific Research Publishing

Advances in Materials Physics and Chemistry, 2020, 10, 151-166
https://www.scirp.org/journal/ampc
ISSN Online: 2162-5328
ISSN Print: 2162-531X

Required CIGS and CIGS/Mo Interface Properties for High-Efficiency $Cu(In, Ga)Se_2$ Based Solar Cells

Soumaïla Ouédraogo[1,2*], Marcel Bawindsom Kébré[1], Ariel Teyou Ngoupo[2], Daouda Oubda[1], François Zougmoré[1], Jean-Marie Ndjaka[2]

[1]Laboratoire de Matériaux et Environnement (LA.M.E)-UFR/SEA, Université Joseph Ki-ZERBO, Ouagadougou, Burkina Faso
[2]Département de Physique, Faculté des Sciences, Université de Yaoundé I, Yaoundé, Cameroun
Email: *ouedraogosoumaila1@gmail.com

How to cite this paper: Ouédraogo, S., Kébré, M.B., Ngoupo, A.T., Oubda, D., Zougmoré, F. and Ndjaka, J.-M. (2020) Required CIGS and CIGS/Mo Interface Properties for High-Efficiency $Cu(In, Ga)Se_2$ Based Solar Cells. *Advances in Materials Physics and Chemistry*, **10**, 151-166.
https://doi.org/10.4236/ampc.2020.107011

Received: June 8, 2020
Accepted: July 21, 2020
Published: July 24, 2020

Abstract

In this work, we have modeled and simulated the electrical performance of CIGS thin-film solar cell using one-dimensional simulation software (SCAPS-1D). Starting from a baseline model that reproduced the experimental results, the properties of the absorber layer and the CIGS/Mo interface have been explored, and the requirements for high-efficiency CIGS solar cell were proposed. Simulation results show that the band-gap, acceptor density, defect density are crucial parameters that affect the performance of the solar cell. The best conversion efficiency is obtained when the absorber band-gap is around 1.2 eV, the acceptor density at 10^{16} cm^{-3} and the defect density less than 10^{14} cm^{-3}. In addition, CIGS/Mo interface has been investigated. It appears that a thin $MoSe_2$ layer reduces recombination at this interface. An improvement of 1.5 to 2.5 mA/cm^2 in the current density (J_{sc}) depending on the absorber thickness is obtained.

Keywords

$Cu(In, Ga)Se_2$, Band-Gap, Acceptor Density, Defect Density, Mo/CIGS-Interface

1. Introduction

The thin-film solar cells represent a considerable hope in the field of PV solar cells. The goal of current research in thin-film solar cells is to develop low-cost, viable, environmentally-friendly materials which is able to compete with the conventional silicon-based structures. Among the thin-film solar cells, those

based on CIGS are very popular because of its very impressive performance. The efficiency of this solar cell has evolved rapidly in recent years due to the maturity of manufacturing techniques. By controlling the benefits of the alkali treatment, the Solar Frontier team achieved a record efficiency of 22.9% [1]. However, CIGS-based solar cells are confronted to serious challenges that could compromise its long-term sustainability. Indium and gallium used in CIGS solar cells and other optoelectronic components are rare [2]. Indium is particularly expensive and it availability can become an issue if the flat panel display industry increases its consumption even more [3]. To overcome this problem, several alternatives are proposed. The replacement of indium and gallium with more abundant, less expensive and more environmentally friendly metals such as zinc and tin has been proposed as an alternative. The best CZTS-based solar cell cells obtained from these substitution metals showed an efficiency of 12.6% [4], far from the performance of CIGS-based cells. The reduction of the CIGS layer thickness appears to be a viable track. If this thickness could be reduced, the use of indium and gallium will be considerably reduced and therefore the deposition time [5]. However, it was argued that reducing the thickness of the absorber below 1 μm leads to a loss of performances resulting from the increase of free-carrier and defect density [5] [6] [7]. The most important loss in the electrical parameters is the short-circuit current which reduces the cell efficiency due to the insufficiency CIGS absorption coefficient, the excessive absorption of the molybdenum layer and the stronger impact of the back contact recombination [5] [7]. In order to develop engineering adapted to ultra-thin absorbers, it is necessary to elucidate the impact of sensitive parameters in the absorber and Mo/CIGS interface properties on the electrical parameters and their evolution with the absorber thickness.

In this paper, SCAPS-1D [8] simulation software was used to investigate CIGS-based solar cells. Starting from a model that reproduces the experimental results, the simulation allowed us to highlight how band-gap, absorber bulk defect density and the Mo/CIGS interface affect the electrical parameters in relation to the absorber thickness.

2. Device Structure

The structure of the simulated solar cell consists of several layers: (Ni/Al)/MgF_2/ZnO:B/i-ZnO/OVC/CIGS/Mo/Substrate. The Mo is sputtered on a subtract, generally soda glass. Several other substrates have been experimented such as stainless steel [9], industrial steel [10], aluminum foil [11], titanium foil [12], polyimide substrates [13]. However, the best performances have been obtained with soda glass [1]. The importance of the soda glass was discussed in terms of good thermal expansion as well as the leakage of impurities such as Na during the CIGS layer deposition [14]. Then, the CIGS absorber is deposited on the Mo by co-evaporation. A thin CdS layer is deposited by chemical bath deposition (CBD) on the CIGS layer to form the p-n junction. In general, an intermediate composition layer is formed at the CdS/CIGS interface. This layer called surface

defect layer (SDL) or ordered vacancy compound (OVC) is related to the atomic inter-diffusion and is supposed to be advantageous to the performance of the solar cell under some conditions [15]. A ZnO intrinsic layer (i-ZnO) and boron-doped ZnO (ZnO:B) layer are deposited on the top of the buffer layer. These two layers are commonly referred to as transparent conductive oxide (TCO), because of their wide band gap which makes them transparent to most of the solar spectrum. The TCO is covered with an antireflection layer MgF_2, which increases the absorption of photons in the absorber.

3. Numerical Modeling

The complexity of the solar cell design increases when efficiency enhancement concepts are considered and computer-aided design becomes necessary for novel semiconductor device development and optimization. Using powerful device simulator is an important strategy to better understand the degree of the performance enhancement that can be provided by these new device structures. Computational analysis was performed using the one-dimensional simulation program SCAPS. Given the proper device structure, values of material parameters and initial conditions, SCAPS program calculates the internal electrical parameters of CIGS solar cells by solving the system of semiconductor equation based on Poisson equation, electrons and holes continuity equations by coupled method of Newton-Rapson. Recombination currents are calculated with the Shockley-Read-Hall (SRH) model for bulk defects and an extension of the SHR model for interface defects. A deeper insight into the effect of the material properties such as doping concentration, free carrier mobilities, band-gap, and structural properties such as different layers and layers thicknesses on device performance can be obtained by the simulation. The material parameters used as the inputs are selected based on the values reported in literature [16] [17] [18]. The semiconductor properties of the intrinsic ZnO:B, i-ZnO, CdS, OVC and CIGS layers used as the input parameters for the simulations are given in **Table 1**.

All the layers are polycrystalline and therefore contain a large number of different defects. In our model, one type of single level defects is introduced in each layer. These are all compensating defects positioned at the intrinsic level which is close to mid-gap. Neutral interface defects for recombination were also positioned at mid-gap. Neutral cross-sections were selected in the range 10^{-18} - 10^{-15} cm^2, while attractive ones were selected in the range 10^{-13} - 10^{-12} cm^2. To pin the Fermi level at the interface level OVC/CdS, donor defects were placed 0.2 eV below the conduction band. These have small capture cross-sections to separate between pinning and the recombination parameters of the OVC layer [17]. The OVC layer parameters are similar to those of bulk CIGS except its band-gap, shallow donor density, and low carrier mobility.

The introduction of Ga into the absorber layer to form the CIGS alloy results in a widening of the band-gap from 1.02 eV to 1.67 eV which are respectively the gap of the CIS and the CGS and Equation (1) is used to adjust the band-gap according to the Ga-content ($x = \mathrm{Ga}/(\mathrm{In}+\mathrm{Ga})$) [19]

Table 1. Input parameters values for the simulation of CIGS solar cells with SCAPS-1D.

Layer Properties					
	CIGS	OVC	CdS	i-ZnO	ZnO:B
Layer thickness (nm)	Variable	Variable	50	200	400
Layer band-gap: E_g (eV)	Variable	Variable	2.4	3.3	3.3
Electrons affinity: χ (eV)	4.5	Variable	4.45	4.55	4.55
Dielectric relative permittivity: $\varepsilon/\varepsilon_0$	13.6	13.6	10	9	9
Conduction band effective density of states: N_c (cm^{-3})	2.2×10^{18}	2.2×10^{18}	1.3×10^{18}	3.1×10^{18}	3×10^{18}
Valence band effective density of state: N_v (cm^{-3})	1.5×10^{19}	1.5×10^{19}	9.1×10^{18}	1.8×10^{19}	1.8×10^{19}
Electron thermal velocity: v_e (cm/s)	3.9×10^{7}	3.9×10^{7}	3.1×10^{7}	2.4×10^{7}	2.4×10^{7}
Hole thermal velocity: v_h (cm/s)	1.4×10^{7}	1.4×10^{7}	1.6×10^{7}	1.3×10^{7}	1.3×10^{7}
Electron mobility: μ_e (cm^2/Vs)	100	variable	72	100	100
Hole mobility: μ_h (cm^2/Vs)	12.5	1.25	20	31	31
Doping concentration (cm^{-3})	2.10^{16}	variable	5×10^{17}	10^{17}	10^{20}
Bulk defect properties					
Defect density and type: N (cm^{-3})	Variable (D)	Variable (D)	5×10^{16} (A)	1016 (A)	10^{16} (A)
Capture cross section electrons: σ_e (cm^2)	10^{-15}	10^{-13}	10^{-15}	10^{-15}	10^{-15}
Capture cross section holes: σ_h (cm^2)	10^{-11}	10^{-15}	5×10^{-13}	5×10^{-13}	5×10^{-13}
Interface properties					
Interface state	CIGS/OVC		OVC/CdS		
Interface conduction band offset: ΔEc (eV)	0.3		0.0		
Defect density and type: N (cm^{-2})	10^{11} (Neutral)		3×10^{13} (Neutral)		

$$E_g\left(\text{eV}\right) = 1.02 + 0.67x + b \cdot x\left(x-1\right) \quad (1)$$

where b is the optical bowing coefficient [19]. The variation in Ga-content in the absorber also affects different material parameters such the conduction band [19], absorption coefficient [20] [21], electron affinity [22], hole mobility [23], net carrier concentration [23] [24], defect density [25]. All these parameters have been calculated according the Ga-content or taken from the literature [20]-[25]. The absorption file used in the simulation were calculated over the entire Ga-content using the equation $\alpha = 2\pi k/\lambda$ [20], where the optical contact k as function of Ga-content is extracted over the wavelength (λ) between 300 and 1300 nm from Palson's and Alonso's papers [20] [21] and is shown in **Figure 1(b)**. The band alignment at the interface between the OVC and the 1.15 eV CIGS layers is set at 0.3 eV [26] [27], guided by experimental results. The default illumination spectrum is set to the global AM1.5 standard for terrestrial solar cell measurement. The series resistance and shunts resistance have been adjusted

according to Ga-content [28], and the temperature is set at 300 K. The equivalent band diagram calculated in thermodynamic equilibrium condition is given in **Figure 1(a)**. The J-V characteristic and quantum efficiency are represented in **Figure 1(c)** and **Figure 1(d)** respectively for $x = 0.3$ and compared to the experimental results [17]. This step is very important in numerical simulation, since it avoids outliers. There is a good similarity between the simulated results and the experimental results and thus validates our model.

4. Results and Discussion

4.1. Effect of the Absorber Band-Gap

The band-gap of the absorber layer is an important variable to enhance the performance of the solar cells. The effects of the increase in the absorber's band-gap on the electrical parameters for different thicknesses are shown in **Figure 2**. The main effects of increasing Ga-content in the absorber are the decrease in short-circuit current density (J_{sc}) and the increase in open-circuit voltage (V_{oc}) [19] [29]. It can be seen that the open circuit voltage (V_{oc}) (**Figure 2(a)**) of the device increases with the Ga-content but not proportionally. For high Ga-contents, although the band-gap increases, the open circuit voltage (V_{oc}) remains relatively constant due to the increase in the recombination rate of charge carriers especially in the space charge region (SCR). The limitation of V_{oc} may be due to defects that increase with the gallium rate [25]. The open circuit voltage is almost independent of the absorber thickness.

The short-circuit current density (**Figure2(b)**) decreases with the absorber's band-gap. This decrease is especially important when the absorber thickness is reduced. This decrease can be attributed to the reduction in the generation rate at the p-n junction due to the decrease in absorption [30] and the increase in recombination at the rear contact when the thickness is significantly reduced [7]. The efficiency (**Figure 2(c)**) of the solar cell as well as the fill factor (FF) (**Figure 2(d)**) increase with the band-gap and the best performance is obtained for $1.2 < E_g < 1.3$ eV. Above this value, the overall performance of the solar cell begins to drop. These results are consistent with the experimental and numerical results obtained from other simulation software [24] [31] [32]. Experimentally, the best CIGS based solar cells are obtained with a Ga-content around $x = 0.3$, corresponding to a $E_g = 1.2$ eV [24]. For a gallium rate x exceeding this value, a drastic decrease in the solar cell's performance is observed. The theoretical estimation of the optimal band-gap energy to achieve the best performance in the photovoltaic devices is in the range of 1.4 to 1.5 eV for the solar spectrum of AM1.5G [30]. The reason why CIGS-based solar cells are less efficient in this range are still poorly understood but all the evidence suggests that the defect level in the absorber depends on the Ga-content and its position moves to the center of band-gap (mid-gap) with the Ga-content which reduces V_{oc} [33] (section 4.3). The new record of 22.9% was achieved by reducing the V_{oc} deficit from the reduction of absorber defect density [1].

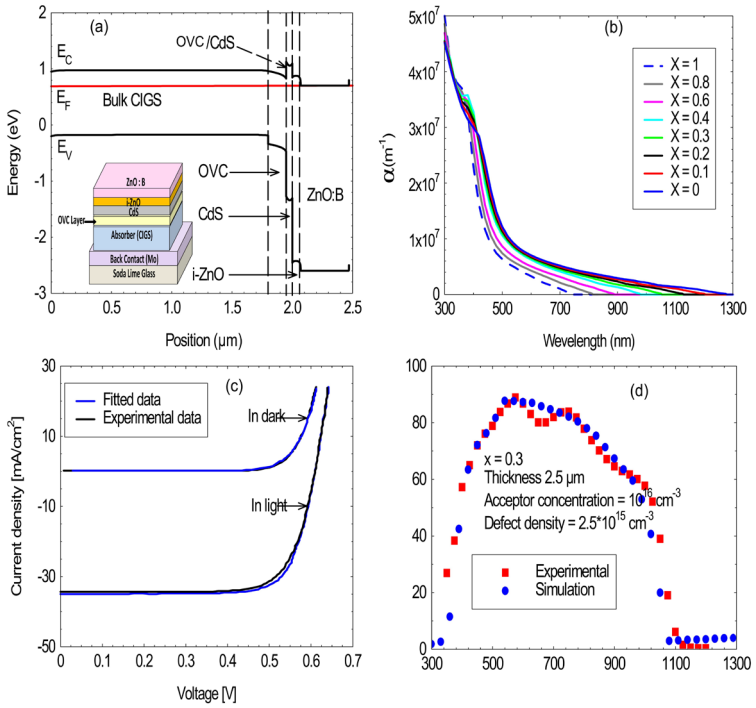

Figure 1. (a) Energy band diagram of CIGS solar cell calculated under thermodynamic equilibrium condition. Inset: CIGS cell structure with the OVC layer at the CdS/CIGS interface; (b) Absorption coefficients versus wavelength used for the simulations from [20] [21]. (c) and (d) J-V characteristic and quantum efficiency compared to experimental results.

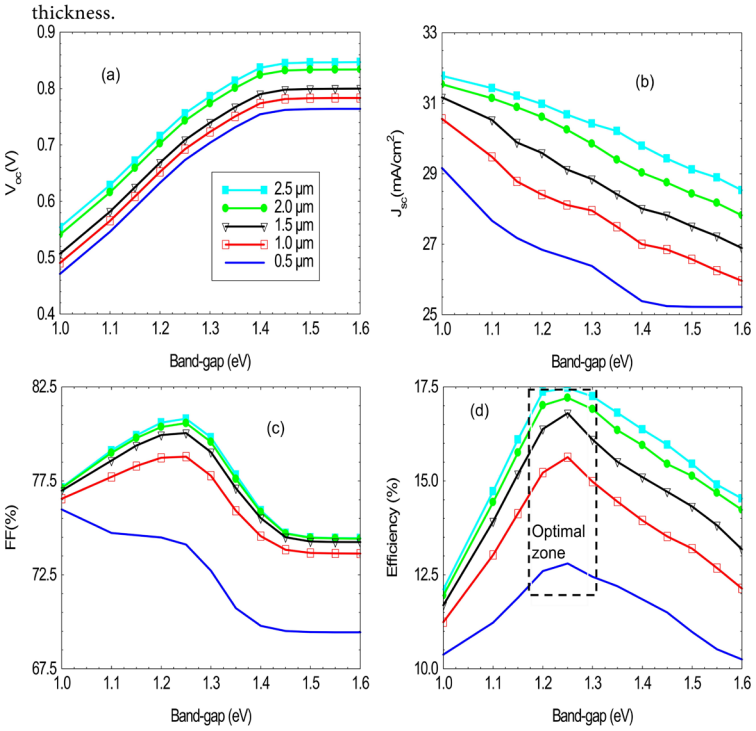

Figure 2. Influence of the increase of the band-gap of the absorber on the electrical parameters (J_{sc}, V_{oc}, FF, Efficiency) according to the thickness of the absorber.

4.2. Effect of Acceptor Concentration

Many impurities during the growth of the absorber are likely to increase the density of acceptors within it. The most common case is the doping of the absorber with the sodium that diffuses from the soda glass substrate. The increase of the sodium doping in the absorber results in an improvement of the open-circuit voltage (V_{oc}) [34]. In addition, the best cells produced nowadays use an alkali post-treatment such as potassium (K) [35] [36], Cs [1]. Several material and device characterizations performed to illuminate the effects of the alkali treatment showed an increased free carrier concentration and reduced carrier recombination throughout the whole absorber film contributed to the improved performance [1]. However, it is recommended to control dopants to optimize the performance of the device since, at high levels, they could reduce mobility and consequently, the lifetime of the charge carriers. In the case of dopants from the substrate, the control is ensured by a barrier (e.g. Al_2O_3) between the molybdenum and the substrate [37] [38].

Figure 3 shows the influence of acceptor density on V_{oc}, J_{sc}, FF and efficiency, for the various thicknesses of the absorber. The open circuit voltage (V_{oc}) (**Figure 3(a)**) increases with the acceptor density and reaches a maximal value when the acceptor concentration is 10^{16} cm^{-3}. Above this value, V_{oc} becomes independent of doping regardless of the absorber thickness. The increase of acceptor concentration of absorber can enhance the built-in electric field of solar cell, which is beneficial to the V_{oc}.

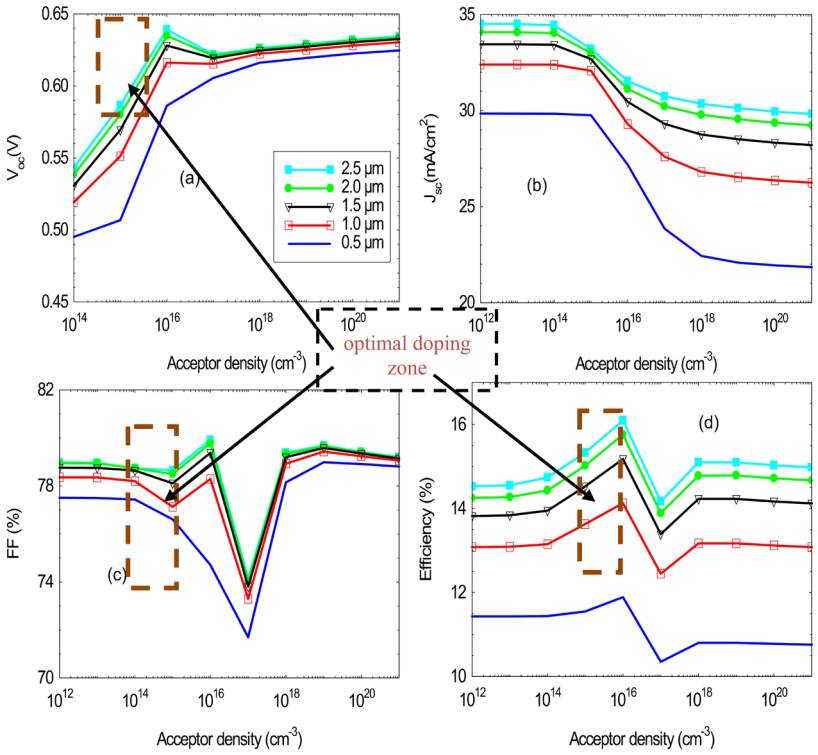

Figure 3. Evolution of the electrical parameters of the solar cell as function of acceptor concentration for different absorber layer thickness.

This increase is in agreement with the experimental results which promote the beneficial effects of impurities such as sodium on V_{oc}. The Short-circuit current density (J_{sc}) (**Figure 3(b)**) decreases with increasing the acceptor density, this decrease is particularly important when the absorber is ultra-thin (<1 μm). The increase in the acceptors density affects the charge carrier mobility, enhances the band-to-band recombination of photo-generated carrier and therefore a deficit in the collection of charge carriers. In addition, Mo/CIGS interface recombination is predominant in ultra-thin absorber, which reduces J_{sc}. The fill factor (**Figure 3(c)**) is less affected for doping level lower than 10^{14} cm^{-3}. However, an improvement of FF is obtained between 10^{15} cm^{-3} et 10^{16} cm^{-3} and reaches a peak at 10^{16} cm^{-3}. Above this value, the increase of acceptor concentration has a negative effect on FF. Fluctuation in V_{oc}, J_{sc} and FF affect the cell's efficiency (**Figure 3(d)**). The best performance is obtained for doping level around 10^{16} cm^{-3}. The simulated results show that the increase of acceptor density in the absorber improves CIGS solar cells performance. However, it is necessary to pay attention to the possible decreases of J_{sc}, FF and efficiency due to enhanced recombination of charge carriers.

4.3. Effect of Absorber Defect Concentration

Defects in the CIGS layer have a crucial role in the cell's performance. For the improvement of CIGS based solar cells device, it is important to understand the impact of the absorber quality on the cell performance and the critical range of defect density on the electrical parameters. The amount of Ga added to the alloy not only influences the band-gap energy but also the transport mechanism and the defects in the absorber [25] [39]. Many studies have shown that the quality of the absorber is the origin of the low performance of CIGS with a high Ga-content [1] [25] [29]. Hanna *et al.* has established a correlation between the Ga-content, absorber bulk defect densities and the solar cells performances as indicated in Equation (2) [25].

$$E_g - qV_{oc} = AkT\ln\left(\frac{j_{00}}{j_{sc}}\right)\alpha A\ln N \tag{2}$$

where q denotes the elementary charge, kT the thermal energy, A the diode ideality factor, j_{sc} the short circuit current and j_{00} a prefactor proportional to the absorber bulk defect density N. This equation demonstrated that bulk defects limit the open circuit voltage of CIGS solar cells in the hole composition range (x = 0 - 1). The simulation was carried out with all parameters constant to better understand the effects of defects. A Gaussian-shaped donors level have been introduced in the bulk of the absorber at an energy above the valence band edge with a characteristic energy width of 0.1 eV. **Table 2** shows the energy level of the defect with respect to the valence band on the electrical parameters. As can be seen, the energetic position of defects has a very important influence on the recombination mechanism. The defects are more harmful at 0.6 eV, *i.e.* close to mid-gap.

Table 2. Dependence of the absorber defect level on the electrical parameters.

Defect level (eV)	0.2	0.4	0.6	0.8
V_{oc} (V)	0.6313	0.6282	0.6281	0.6290
J_{sc} (mA/cm^2)	34.67	34.36	34.35	34.44
FF (%)	73.59	73.46	73.45	73.51
Efficiency (%)	16.11	15.86	15.85	15.93

Thereafter, we use this worst scenario to better elucidate the effect of the absorber defect density as shown in **Figure 4**.

The electrical parameters are less sensitive to defects when they are less than 10^{14} cm^{-3} regardless of the thickness of the absorber. Per account, beyond 10^{14} cm^{-3}, all parameters drop drastically. This suggests that a high defect density may be the origin of the poor performance in CIGS cells with a high Ga content. The record efficiency of 22.9% obtained by the Solar Frontier team was correlated to an improvement of the absorber quality [1].

4.4. Mo/CIGS Interface Optimization

At the Mo/CIGS interface an ohmic contact with a low contact resistance is desired in order to extract efficiently the photo-generated charge carriers from the CIGS absorber [40]. It is generally observed that a $MoSe_2$ layer is formed at the Mo/CIGS interface during the deposition of the CIGS absorber on the Mo by the selenization of Cu-In-Ga precursor. Several factor can be responsible for the $MoSe_2$ layer: the sputtering pressure of Mo [41], Na content from soda glass [42] [43] [44], the selenization temperature [45]. Many studies are unanimous that the $MoSe_2$ layer contributes to the improvement of adhesion at the CIGS/Mo interface [44] [46]. In addition, the $MoSe_2$ layer at the Mo/CIGS interface acts in a beneficial way by changing the Mo/CIGS hetero-contact from Schottky to an ohmic type contact [40] [46] [47].

Generally, the Mo/CIGS interface is a high recombination area, especially for ultra-thin absorbers. The $MoSe_2$ layer with its 1.4 eV band-gap could be a good electron reflector, very important to reduce Mo/CIGS interface recombination [45] [48].

However, an optimal $MoSe_2$ layer thickness is required since a very thick $MoSe_2$ limits the current collecting ability of the back electrode due to the high resistivity of $MoSe_2$ (10^1 - 10^4 Ωcm) and hence deteriorating the electrical parameters [49] [50]. An optimization of the $MoSe_2$ layer thickness is therefore required to give it its role as an electron reflector. The $MoSe_2$ layer parameters used in the simulation are represented in **Table 3**. The equivalent band-diagrams with and without the $MoSe_2$ layer are shown in **Figure 5(a)** and **Figure 5(b)** respectively. The comparison of the J-V characteristic and the quantum efficiency in these two configurations are represented by **Figure 5(c)** and **Figure 5(d)**.

Table 4 shows the electrical parameters extracted from the J-V characteristic. As can be seen, a thin $MoSe_2$ layer at Mo/CIGS improves the electrical pa-

rameters.

The open circuit voltage (V_{oc}) increases as a result to the passivation of the Mo/CIGS interface defects as in the case of the Al_2O_3 layer [37] [38]. Moreover, there is an improvement in the current density due to a potential barrier at the Mo/CIGS interface that prevents electrons from recombining with the holes. This results in a good collection of charge carriers as shown in **Figure 5(d)**.

To elucidate the advantages or disadvantages of the $MoSe_2$ layer, we performed the simulations by focusing only on its thickness, which seems to be the critical parameters at the Mo/CIGS interface. We have intentionally omitted the open circuit voltage (V_{oc}), since J_{sc} and FF are the most affected by the recombination at the Mo/CIGS interface. **Figure 6(a)** shows the effect of the $MoSe_2$ layer thickness on J_{sc}, FF and the Efficiency as function of the absorber thickness. J_{sc} and FF are almost unaffected by the increase in the thickness of the $MoSe_2$ layer, however, it depends more to the absorber thickness. When the thickness of the absorber is large, interactions between electrons and holes are reduced, which improves the J_{sc}. The FF increases with the $MoSe_2$ layer thickness due to the passivation of the Mo/CIGS interface. Nevertheless, ultra-thin absorbers are more advantageous by the $MoSe_2$ layer thickness. The gain of the electrical parameters is shown in **Figure 6(b)**. This gain was obtained by subtracting the electrical parameters with $MoSe_2$ from those without $MoSe_2$. As can be seen, ΔJ_{sc} increases with the thickness of the $MoSe_2$ layer but also depends on the thickness of the absorber. For ultra-thin absorbers less than 0.8 μm, a 600 nm $MoSe_2$ layer allows a gain between 1.5 and 2.5 mA/cm^2. On the other hand, for absorbers higher than 0.8 μm, the presence of the $MoSe_2$ layer regardless of its thickness becomes critical on the J_{sc}. In this situation, the beneficial effects on the $MoSe_2$ as an electron reflector are less pronounced and become detrimental to the J_{sc}. ΔFF decreases almost linearly with absorber thickness.

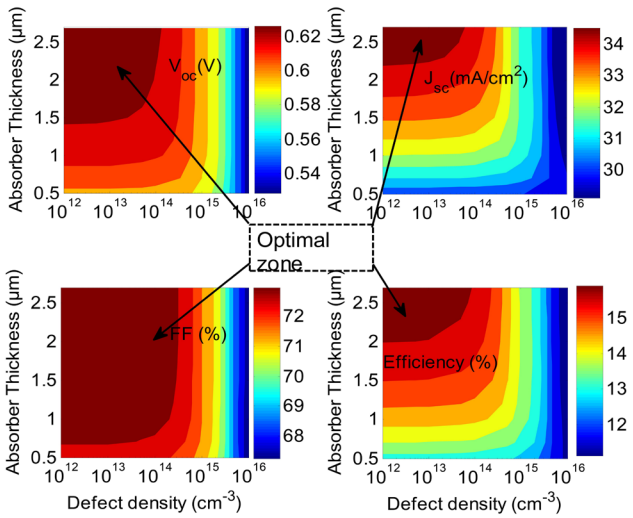

Figure 4. Calculated impact of absorber thickness and total defect density on the electrical parameters: V_{oc}, J_{sc}, FF and Efficiency.

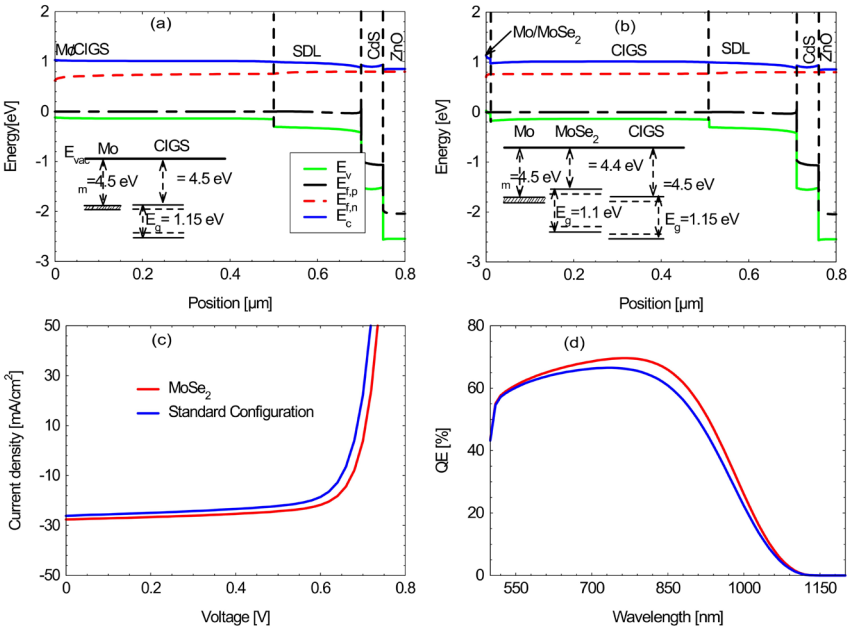

Figure 5. Energy band diagram (a) without $MoSe_2$ layer (standard configuration), (b) With $MoSe_2$ layer. (c) J-V and (d) QE characteristics of both configurations.

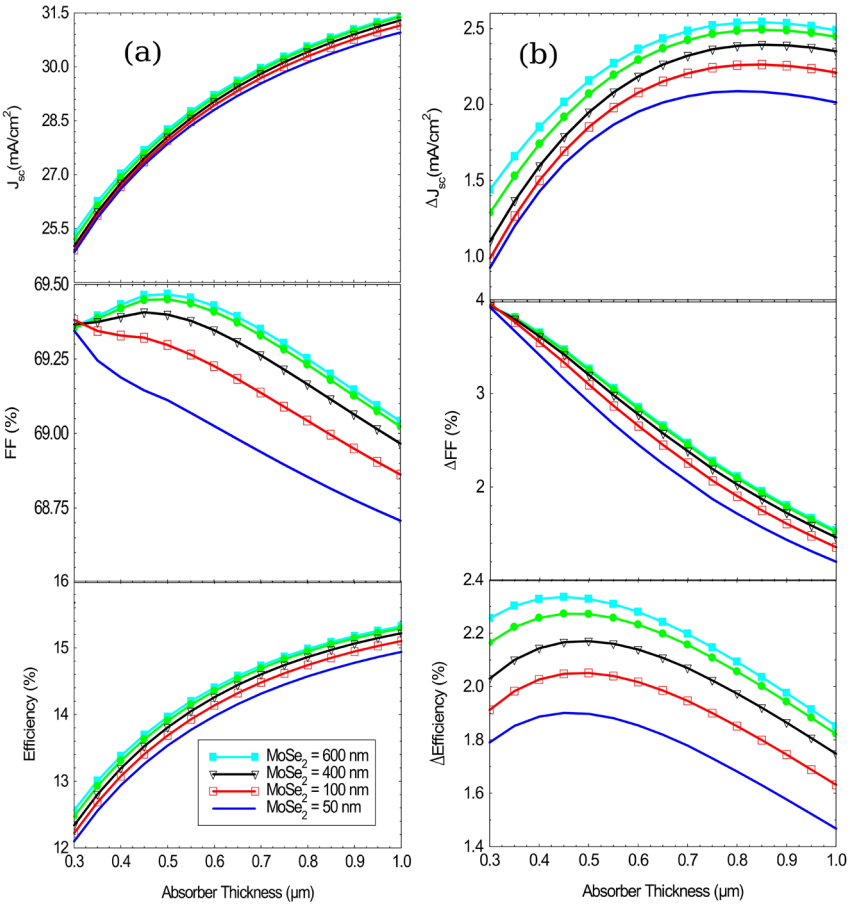

Figure 6. (a) Electrical parameters according to the $MoSe_2$ layer and CIGS absorber thicknesses; (b) gain due to the presence of the $MoSe_2$ layer.

Table 3. $MoSe_2$ input parameters [49] [50].

Parameters	p-$MoSe_2$
Layer thickness (nm)	Variable
Layer band-gap: E_g (eV)	1.1
Electrons affinity: χ (eV)	4.372
Dielectric relative permittivity: $\varepsilon/\varepsilon_0$	13.6
Conduction band effective density of states: N_c (cm^{-3})	2.2×10^{18}
Valence band effective density of state: N_v (cm^{-3})	1.8×10^{19}
Electron thermal velocity: v_e (cm/s)	10^7
Hole thermal velocity: v_h (cm/s)	10^7
Electron mobility: μ_e (cm^2/Vs)	100
Hole mobility: μ_h (cm^2/Vs)	25
Doping concentration (cm^{-3})	1×10^{16}

Table 4. Results from simulation with and without (W/o) $MoSe_2$ layer.

	V_{oc} (V)	J_{sc} (mA/cm^2)	FF (%)	Efficiency (%)
W/o BSF	0.673	26.098	66.22	11.67
$MoSe_2$	0.6943	27.601	68.51	13.13

5. Conclusion

We investigated the requirements to obtain high performance CIGS-based solar cells with SCAPS simulation software. Starting from a baseline model that reproduced the experimental results, we have shown that the achievement of high performance CIGS solar cell requires the optimization of the absorber's properties but also a careful focus on the Mo/CIGS interface. These requirements in the absorber process can be summarized as follows: 1) control the Ga-content to obtain a band-gap between 1.2 eV and 1.3 eV; 2) the acceptor density should be around 10^{16} cm^{-3} and 3) the defect density must be lower than 10^{14} cm^{-3}. The selenization conditions of Cu-In-Ga precursor on the Mo must be adjusted correctly to obtain ultra-thin $MoSe_2$ layer at the Mo/CIGS.

Acknowledgements

The authors acknowledge the use of the SCAPS-1D program developed by Marc Burgelman and colleagues at the University of Gent in all the simulations reported in this article.

Conflicts of Interest

The authors declare no conflicts of interest regarding the publication of this paper.

References

[1] Kato, T., Wu, J.L., Hirai, Y., Sugimoto, H. and Bermudez, V. (2019) Record Effi-

ciency for Thin-Film Polycrystalline Solar Cells Up to 22.9% Achieved by Cs-Treated Cu(In,Ga)(Se,S)$_2$. *IEEE Journal of Photovoltaics*, **9**, 325. https://doi.org/10.1109/JPHOTOV.2018.2882206

[2] Schock, H.-W. and Noufi, R. (2000) CIGS-Based Solar Cells for the Next Millennium. *Progress in Photovoltaics*: *Research and Applications*, **8**, 151-160. https://doi.org/10.1002/(SICI)1099-159X(200001/02)8:1<151::AID-PIP302>3.0.CO;2-Q

[3] Ramanathan, K., Noufi, R., To, B., Young, D.L., Bhattacharya, R., Contreras, M.A., Dhere, R.G. and Teeter, G. (2006) Processing and Properties of Sub-Micron CIGS Solar Cells. *Photovoltaic Energy Conversion Conference Record of the IEEE*, Vol. 1, 380-383. https://doi.org/10.1109/WCPEC.2006.279469

[4] Wang, W., Winkler, M.T., Gunawan, O., Gokmen, T., Todorov, T.K., Zhu, Y. and Mitzi, D.B. (2014) Device Characteristics of CZTSSe Thin-Film Solar Cells with 12.6% Efficiency. *Advanced Energy Materials*, **4**, 1-5. https://doi.org/10.1002/aenm.201301465

[5] Lundberg, O., Bodegard, M., Malmstrom, J. and Stolt, L. (2003) Influence of the Cu(In,Ga)Se$_2$ Thickness and Ga Grading on Solar Cell Performance. *Progress in Photovoltaics*: *Research and Applications*, **11**, 77-88. https://doi.org/10.1002/pip.462

[6] Gloeckler, M. and Sites, J.R. (2005) Potential of Submicrometer Thickness Cu(In,Ga)Se$_2$ Solar Cells. *Journal of Applied Physics*, **98**, Article ID: 103703. https://doi.org/10.1063/1.2128054

[7] Degrave, S., Burgelman, M. and Nollet, P. (2003) Modelling of Polycrystalline Thin Film Solar Cells: New Features in SCAPS Version 2.3. *Proceedings* 3*rd WCPEC*, Vol. 1, 487-490.

[8] Eisenbarth, T., Caballero, R., Kaufmann, C.A., Eicke, A. and Unold, T. (2012) Influence of Iron on Defect Concentrations and Device Performance of Cu(In,Ga)Se$_2$ Solar Cells on Stainless Steel Substrates. *Progress in Photovoltaics*: *Research and Applications*, **20**, 568-574. https://doi.org/10.1002/pip.2260

[9] Wuerz, R., Eicke, A., Frankenfeld, M., Kessler, F., Powalla, M., Rogin, P. and Yazdani-Assl, O. (2009) CIGS Thin-Film Solar Cells on Steel Substrates. *Thin Solid Films*, **517**, 2415-2418. https://doi.org/10.1016/j.tsf.2008.11.016

[10] Brémaud, D., Rudmann, D., Kaelin, M., Ernits, K., Bilger, G., Döbeli, M., Zogg, H. and Tiwari, A.N. (2007) Flexible Cu(In,Ga)Se$_2$ on Al Foils and the Effects of Al during Chemical Bath Deposition. *Thin Solid Films*, **515**, 5857-5861. https://doi.org/10.1016/j.tsf.2006.12.152

[11] Kaufmann, C.A., Neisser, A., Klenk, R. and Scheer, R. (2005) Transfer of Cu(In,Ga)Se$_2$ Thin Film Solar Cells to Flexible Substrates Using an *in Situ* Process Control. *Thin Solid Films*, **480**, 515-519. https://doi.org/10.1016/j.tsf.2004.11.067

[12] Urbaniak, A., Igalson, M., Pianezzi, F., Bücheler, S., Chirilă, A., Reinhard, P. and Tiwari, A.N. (2014) Effects of Na Incorporation on Electrical Properties of Cu(In,Ga)Se$_2$-Based Photovoltaic Devices on Polyimide Substrates. *Solar Energy Materials & Solar Cells*, **128**, 52-56. https://doi.org/10.1016/j.solmat.2014.05.009

[13] Contreras, M.A., Egaas, B., Dippo, P., Webb, J., Granata, J., Ramanathan, K., Asher, S., Swartzlander, A. and Noufi, R. (1997) On the Role of Na and Modifications to Cu(In,Ga)Se$_2$ Absorber Materials Using Thin-MF (M = Na, K, Cs) Precursor Layers. *IEEE Photovoltaic Specialists Conference*, Anaheim, 29 September-3 October 1997, 359-362. https://doi.org/10.1109/PVSC.1997.654102

[14] Ouédraogo, S., Zougmoré, F. and Ndjaka, J.M.B. (2014) Computational Analysis of

the Effect of the Surface Defect Layer (SDL) Properties on Cu(In,Ga)Se_2-Based Solar Cell Performances. *Journal of Physics and Chemistry of Solids*, **75**, 688-695. https://doi.org/10.1016/j.jpcs.2014.01.010

[15] Scheer, R. (2011) Towards an Electronic Model for $CuIn_{1-x}Ga_xSe_2$ Solar Cells. *Thin Solid Films*, **519**, 7472-7475. https://doi.org/10.1016/j.tsf.2011.01.092

[16] Petterson, J., Platzer-Björkman, C., Zimmermann, U. and Edoff, M. (2011) Baseline Model of Gradued-Absorber Cu(In,Ga)Se_2 Solar Cells Applied to Cells with $Zn_{1-x}Mg_xO$ Buffer Layers. *Thin Solid Film*, **519**, 7476-7480. https://doi.org/10.1016/j.tsf.2010.12.141

[17] Gloeckler, M., Fahrenbruch, A.L. and Sites, J.R. (2003) Numerical Modeling of CIGS and CdTe Solar Cells: Setting the Baseline. *Proc. 3rd WCPEC*, Vol. 1, 491-494.

[18] Lundberg, O., Edoff, M. and Stolt, L. (2005) The Effect of Ga-Grading in CIGS Thin Film Solar Cells. *Thin Solid Film*, **480-481**, 520-525. https://doi.org/10.1016/j.tsf.2004.11.080

[19] Alonso, M.I., Garriga, M., Durante Rincon, C.A., Hernandez, E. and Leon, M. (2002) Optical Functions of Chalcopyrite $CuGa_xIn_{1-x}Se_2$ Alloys. *Applied Physics A*, **74**, 659-664. https://doi.org/10.1007/s003390100931

[20] Paulson, P.D., Birkmire, R.W. and Shafarman, W.N. (2003) Optical Characterization of $CuIn_{1-x}Ga_xSe_2$ Alloy Thin Films by Spectroscopic Ellipsometry. *Journal of Applied Physics*, **94**, 879. https://doi.org/10.1063/1.1581345

[21] Minemoto, T., Matsui, T., Takakura, H., Hamakawa, Y., Negami, T., Hashimoto, Y., Uenoyama, T. and Kitagawa, M. (2001) Theoretical Analysis of the Effect of Conduction Band Offset of Window/CIS Layers on the Performance of CIS Solar Cells Using Device Simulation. *Solar Energy Material & Solar Cells*, **67**, 83-88. https://doi.org/10.1016/S0927-0248(00)00266-X

[22] Schroeder, D.J., Hernandez, J.L., Berry, G.D. and Rockett, A.A. (1998) Hole Transport and Doping States in Epitaxial $CuIn_{1-x}Ga_xSe_2$. *Journal of Applied Physics*, **83**, 11519. https://doi.org/10.1063/1.366860

[23] Jung, S., Ahn, S., Yun, J.H., Gwak, J., Kim, D. and Yoon, K. (2010) Effects of Ga Contents on Properties of CIGS Thin Films and Solar Cells Fabricated by Co-Evaporation Technique. *Current Applied Physics*, **10**, 990-996. https://doi.org/10.1016/j.cap.2009.11.082

[24] Hanna, G., Jasenek, A., Rau, U. and Schock, H.W. (2001) Influence of the Ga-Content on the Bulk Defect Densities of Cu(In,Ga)Se_2. *Thin Solid Films*, **387**, 71-73. https://doi.org/10.1016/S0040-6090(00)01710-7

[25] Okano, Y., Nakada, T. and Kunioka, A. (1998) XPS Analysis of CdS/$CuInSe_2$ Heterojunction. *Solar Energy Materials and Solar Cells*, **50**, 105. https://doi.org/10.1016/S0927-0248(97)00129-3

[26] Kim, G.Y., Jo, W., Jo, H.J., Kim, D.H. and Kang, J.K. (2015) Macroscopic and Microscopic Electrical Properties of Cu(In,Ga)Se_2 Thin-Film Solar Cells with Various Ga/(In+Ga) Contents. *Current Applied Physics*, **15**, S44-S50. https://doi.org/10.1016/j.cap.2015.04.036

[27] Gloeckler, M. and Sites, J.R. (2005) Band-Gap Grading in Cu(In,Ga)Se_2 Solar Cells. *Journal of Physics and Chemistry of Solids*, **66**, 1891-1894. https://doi.org/10.1016/j.jpcs.2005.09.087

[28] Huang, C.H. (2008) Effects of Ga Content on Cu(In,Ga)Se_2 Solar Cells Studied by Numerical Modeling. *Journal of Physics and Chemistry of Solids*, **69**, 330-334. https://doi.org/10.1016/j.jpcs.2007.07.093

[29] Ouédraogo, S., Zougmoré, F. and Ndjaka, J.M. (2013) Numerical Analysis of Cop-

per-Indium-Gallium-Diselenide-Based Solar Cells by SCAPS-1D. *International Journal of Photoenergy*, **2013**, Article ID: 421076. https://doi.org/10.1155/2013/421076

[30] Contreras, M.A., Mansfield, L.M., Egaas, B., Li, J., Romero, M., Noufi, R., Voigt, E.R. and Mannstadt, W. (2012) Wide Bandgap $Cu(In,Ga)Se_2$ Solar Cells with Improved Energy Conversion Efficiency. *Progress in Photovoltaics*: *Research and Applications*, **20**, 843-850. https://doi.org/10.1002/pip.2244

[31] Heath, J.T., Cohen, J.D., Shafarman, W.N., Liao, D.X. and Rockett, A.A. (2002) Effect of Ga Content on Defect States in $CuIn_{1-x}Ga_xSe_2$ Photovoltaic Devices. *Applied Physics Letters*, **80**, 4540. https://doi.org/10.1063/1.1485301

[32] Ruckh, M., Schmid, D., Kaiser, M., Schäffler, R., Walter, T. and Schock, H.W. (1996) Influence of Substrates on the Electrical Properties of $Cu(In,Ga)Se_2$ Thin Films. *Solar Energy Materials and Solar Cells*, **41**, 335-343. https://doi.org/10.1016/0927-0248(95)00105-0

[33] Jackson, P., Wuerz, R., Hariskos, D., Lotter, E., Witte, W. and Powalla, M. (2016) Effects of Heavy Alkali Elements in $Cu(In,Ga)Se_2$ Solar Cells with Efficiencies Up to 22.6%. *Physica Status Solidi RRL*, **10**, 583-586. https://doi.org/10.1002/pssr.201600199

[34] Kato, T., Handa, A., Yagioka, T., Matsuura, T., Yamamoto, K., Higashi, S., Wu, J.L., Tai, K.F., Hiroi, H., Yoshiyama, T., Sakai, T. and Sugimoto, H. (2017) Enhanced Efficiency of Cd-Free $Cu(In,Ga)(Se,S)_2$ Mini-Module via (Zn,Mg)O Second Buffer Layer and Alkali Metal Post-Treatment. *IEEE Journal of Photovoltaics*, **7**, 1773. https://doi.org/10.1109/JPHOTOV.2017.2745710

[35] Vermang, B., Fjällström, V., Pettersson, J., Salomé, P. and Edoff, M. (2013) Development of Rear Surface Passivated $Cu(In,Ga)Se_2$ Thin Film Solar Cells with Nano-Sized Local Rear Point Contacts. *Solar Energy Materials & Solar Cells*, **117**, 505-511. https://doi.org/10.1016/j.solmat.2013.07.025

[36] Kotipalli, R., Vermang, B., Joel, J., Rajkumar, R., Edoff, M. and Flandre, D. (2015) Investigating the Electronic Properties of Al_2O_3/$Cu(In,Ga)Se_2$ Interface. *AIP Advances*, **5**, Article ID: 107101. https://doi.org/10.1063/1.4932512

[37] Turcu, M., Kötschau, I.M. and Rau, U. (2002) Composition Dependence of Defect Energy and Band Alignments in the $Cu(In_{1-x}Ga_x)(Se_{1-y}S_y)_2$ Alloy System. *Journal of Applied Physics*, **91**, 1391. https://doi.org/10.1063/1.1432126

[38] Klinkert, T., Theys, B., Patriarche, G., Jubault, M., Donsanti, F., Guillemoles, J.-F. and Lincot, D. (2016) New Insights into the Mo/$Cu(In,Ga)Se_2$ Interface in Thin Film Solar Cells: Formation and Properties of the $MoSe_2$ Interfacial Layer. *The Journal of Chemical Physics*, **145**, Article ID: 154702. https://doi.org/10.1063/1.4964677

[39] Zhu, X., Zhou, Z., Wang, Y., Zhang, L., Li, A. and Huang, F. (2012) Determining Factor of $MoSe_2$ Formation in $Cu(In,Ga)Se_2$ Solar Cells. *Solar Energy Materials & Solar Cells*, **101**, 57-61. https://doi.org/10.1016/j.solmat.2012.02.015

[40] Rostan, P.J., Mattheis, J., Bilger, G., Rau, U. and Werner, J.H. (2005) Formation of Transparent and Ohmic ZnO:Al/$MoSe_2$ Contacts for Bifacial $Cu(In,Ga)Se_2$ Solar Cells and Tandem Structures. *Thin Solid Films*, **480-481**, 67-70. https://doi.org/10.1016/j.tsf.2004.11.001

[41] Lin, Y.C., Hong, D.H., Hsieh, Y.T., Wang, L.C. and Hsu, H.R. (2016) Role of Mo:Na Layer on the Formation of $MoSe_2$ Phase in $Cu(In,Ga)Se_2$ Thin Film Solar Cells. *Solar Energy Materials & Solar Cells*, **155**, 226-233. https://doi.org/10.1016/j.solmat.2016.06.024

[42] Wurz, R., Marron, D.F., Meeder, A., Rumberg, A., Babu, S.M., Niedrig, T.S., Bloeck, U., Bischoff, P.S. and Steiner, M.C.L. (2003) Formation of an Interfacial $MoSe_2$ Layer in CVD Grown $CuGaSe_2$ Based Thin Film Solar Cells. *Thin Solid Films*, **431-432**, 398. https://doi.org/10.1016/S0040-6090(03)00261-X

[43] Lin, Y.C., Shen, M.T., Chen, Y.L., Hsu, H.R. and Wu, C.H. (2014) A Study on $MoSe_2$ Layer of Mo Contact in Cu(In,Ga)Se2 Thin Film Solar Cells. *Thin Solid Films*, **570**, 166-171. https://doi.org/10.1016/j.tsf.2014.04.016

[44] Wada, T., Kohara, N., Nishiwaki, S. and Negami, T. (2001) Characterization of the Cu(In,Ga)Se_2/Mo Interface in CIGS Solar Cells. *Thin Solid Films*, **387**, 118-122. https://doi.org/10.1016/S0040-6090(00)01846-0

[45] Abou-Ras, D., Kostorz, G., Bremaud, D., Klin, M., Kurdesau, F.V., Tiwari, A.N. and Dfbeli, M. (2005) Formation and Characterisation of $MoSe_2$ for Cu(In,Ga)Se_2 Based Solar Cells. *Thin Solid Films*, **480-481**, 433-438. https://doi.org/10.1016/j.tsf.2004.11.098

[46] Kohara, N., Nishiwaki, S., Hashimoto, Y., Negami, T. and Wada, T. (2001) Electrical Properties of the Cu(In,Ga)Se_2/$MoSe_2$/Mo Structure. *Solar Energy Materials & Solar Cells*, **67**, 209-215. https://doi.org/10.1016/S0927-0248(00)00283-X

[47] Pouzet, J. and Bernede, J.C. (1990) $MoSe_2$ Thin Film Synthesized by Solid State Reactions between Mo and Se Thin Films. *Revue de Physique Appliquée*, **25**, 807-815. https://doi.org/10.1051/rphysap:01990002508080700

[48] Duchatelet, A., Savidand, G., Vannier, R.N. and Lincot, D. (2013) Optimization of $MoSe_2$ Formation for Cu(In,Ga)Se_2-Based Solar Cells by Using Thin Superficial Molybdenum Oxide Barrier Layers. *Thin Solid Films*, **545**, 94-99. https://doi.org/10.1016/j.tsf.2013.07.038

[49] Cozza, D., Ruiz, C.M., Duche, D., Simon, J.J. and Escoubas, L. (2016) Modeling the Back Contact of $Cu_2ZnS_nSe_4$ Solar Cells. *IEEE Journal of Photovoltaics*, **6**, 1296. https://doi.org/10.1109/JPHOTOV.2016.2576678

[50] Minbashi, M., Omrani, M.K., Melarian, N. and Kim, D.H. (2017) Comparison of Theoretical and Experimental Results for Band-Gap-Graded CZTSSe Solar Cell. *Current Applied Physics*, **17**, 1238-1243. https://doi.org/10.1016/j.cap.2017.06.003